Scalar-Based Finite Element Modelling of 3D Eddy Currents in Thin Moving Conducting Sheets

N. Allen D.Rodger H.C. Lai and P.J.Leonard
University of Bath, Bath Avon BA2 7AY, U.K.

***Abstract*—A new set of formulations is presented for the 3D eddy current finite element analysis of thin moving conducting sheets. The conducting sheet, moving at a constant linear velocity in the direction of the sheet plane, is modelled using two scalar quantities, T and the normal component of the magnetic flux density. The second scalar, $\mathbf{B}\cdot\mathbf{n}$, is introduced to maintain a second order partial differential equation system. Scalar potentials are used to model the nonconducting regions. This scheme, implemented for time-harmonic cases, is compared with the more usual $\mathbf{A}-\psi$ method using a computer model, and force predictions agree favourably. In the DC limit, it is possible to eliminate the T variable, thereby retaining only the $\mathbf{B}\cdot\mathbf{n}$ scalar in the sheet description. Two experimental test problems serve to illustrate drag and lift force predictions obtained using the two new schemes, $T-\mathbf{B}\cdot\mathbf{n}-\psi$ and $\mathbf{B}\cdot\mathbf{n}-\psi$, and the more usual moving $\mathbf{A}-\psi$ formulation.**

Introduction

A number of electromagnetic devices contain geometries which prove to be challenging when modelled using finite elements. One type of complexity may be a physical dimension which is significantly smaller than the others. For example, a design of maglev coil-track systems may involve the use of relatively thin track sheets of finite widths and extensive lengths. The finite elements used in the modelling discretization can present such a high aspect ratio that accuracy is deteriorated. In order to limit the aspect ratio to reasonable values, it may be necessary to significantly increase the number of elements, sometimes beyond available computer capabilities.

A new finite element formulation is presented for 3D eddy current modelling of thin linear conducting sheets moving at a constant linear velocity in the direction of the sheet planes. Two scalar variables, T and the normal component of $\mathbf{B}$, are used to describe the conducting sheet region, while scalar potentials are used to model sources and non conducting regions. The scheme is more economical for appropriate problems than the more general three-component magnetic vector potential used in the moving $\mathbf{A}-\psi$ method [1].

Manuscript received July 10, 1995

The new schemes may be used in situations where the moving conductor thickness is less than the skin depth of the material, this allows the assumption that current density is constant across the thickness of the conducting region, so that conducting sheets can be modelled as surface elements. This scheme may lead to a considerably more accurate solution than the $\mathbf{A}-\psi$ method for very thin sheets since the material thickness is only used as a parameter and no thin elements are present in the mesh. Furthermore, in the DC limit, it is demonstrated that it is possible to eliminate the T variable, thereby retaining only the $\mathbf{B}\cdot\mathbf{n}$ variable in the sheet description.

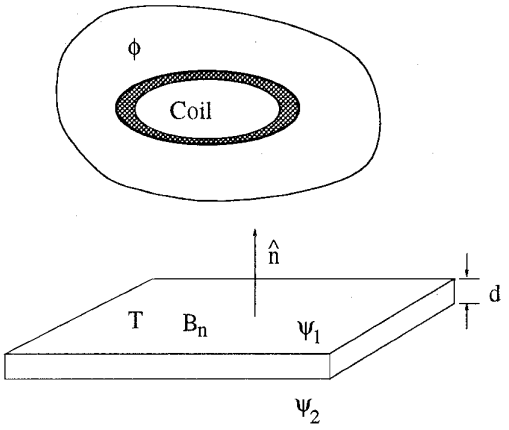

Fig. 1. Showing the sheet variables

Finite Element Formulations

The moving eddy current problem is partitioned into three regions, as shown in Fig. 1. Regions without eddy currents are modelled using the total and reduced magnetic scalar potentials, as is fully described in [2]. Both scalar potentials give rise to a Laplacian-type equation of the form

$$\nabla\cdot\mu\nabla\psi = 0. \tag{1}$$

The first of the new schemes uses two scalars, T and the normal component of the flux density $\mathbf{B}\cdot\mathbf{n}$ to model the thin sheet, while the second is restricted to DC problems and only requires the $\mathbf{B}\cdot\mathbf{n}$ scalar.

$T - \mathbf{B}\cdot\mathbf{n}$ *Formulation*

For conducting sheets which are thin compared to the skin depth of the material, it is reasonable to assume a uniform distribution of the eddy currents across the thickness of the sheet. Therefore, as described in [3], a surface current density is defined as

$$\mathbf{K} = \mathbf{J}d, \tag{2}$$

where d is the thickness of the sheet.

Since $\mathbf{K}$ varies only on the sheet plane, it is economical to represent it in terms of a scalar quantity T such as

$$\mathbf{K} = \frac{\partial}{\partial t}(\nabla T \times \mathbf{n}). \tag{3}$$

If the sheet moves at a constant linear velocity $\mathbf{u}$ in the direction of the sheet plane, then the Minkowski transformation can be applied to bring the moving body to rest through the addition of a motional emf term $\mathbf{u}\times\mathbf{B}$ and the expression for the surface current becomes

$$\mathbf{K}_{eff} = \frac{\partial}{\partial t}(\nabla T \times \mathbf{n}) + d\sigma(\mathbf{u}\times\mathbf{B}), \tag{4}$$

where σ is the sheet conductivity.

The thin sheet is now modelled as a surface and the appropriate interface conditions are applied.

Interface Conditions at the Sheet Surface

At a point on the surface, the scalar quantity T can be related to ψ_1 and ψ_2 on either side of the surface using the condition on $\mathbf{H}\times\mathbf{n}$:

$$\nabla\psi_1 \times \mathbf{n} - \nabla\psi_2 \times \mathbf{n} = \frac{\partial}{\partial t}(\nabla T \times \mathbf{n}) + d\sigma(\mathbf{u}\times\mathbf{B}) \tag{5}$$

Dividing (5) by σd, performing the curl, and then extracting the normal component yields

$$\begin{aligned}\left[\nabla\times\tfrac{1}{\sigma d}(\nabla\psi_1 \times \mathbf{n} - \nabla\psi_2 \times \mathbf{n})\right]\cdot\mathbf{n} \quad &= \\ \left[\nabla\times\tfrac{1}{\sigma d}\tfrac{\partial}{\partial t}(\nabla T \times \mathbf{n})\right]\cdot\mathbf{n} - (\mathbf{u}\cdot\nabla)(\mathbf{B}\cdot\mathbf{n}).\end{aligned} \tag{6}$$

An expression for $\mathbf{B}\cdot\mathbf{n}$ in terms of T is obtained from Faraday's law and is of the form:

$$\mathbf{B}\cdot\mathbf{n} = -\left[\nabla\times\frac{1}{\sigma d}(\nabla T\times\mathbf{n})\right]\cdot\mathbf{n} \tag{7}$$

Equation (7) identifies the new variable $\mathbf{B}\cdot\mathbf{n}$ independently, since its inclusion into (6) would yield a third order term and therefore violate the continuity constraints when applying the finite element method.

Continuity of $\mathbf{B}\cdot\mathbf{n}$ across the thickness of the sheet is ensured by recasting the usual surface integral terms of $\mathbf{B}\cdot\mathbf{n}$ arising from the Galerkin treatment of (1) in terms of T using (7). Furthermore, no jump due to surface currents is possible at the edge of the sheet, so $\psi_1 = \psi_2$ is set on the periphery of the sheet.

It is important to note that (4) is not a complete description of current since the assumption of divergenceless $\mathbf{J}$ for quasimagnetostatics is not respected. An electric scalar term (∇V) is required to ensure that the component of $\mathbf{J}$ coming out of the plate edge is zero. However, since the formulation includes taking the curl of (4), the electric scalar term vanishes, as the curl of grad is identically zero. Furthermore, since the surface current density can be expressed in terms of the scalar potentials on either side of the sheet, the requirement for V in representing the current is eliminated.

The Galerkin weighted residual method is applied and the resulting asymmetric $\psi_1, \psi_2, T, \mathbf{B}\cdot\mathbf{n}$ system of equations is solved using a preconditioned biconjugate gradient scheme.

$\mathbf{B}\cdot\mathbf{n}$ *Formulation*

At DC, (6) reduces to

$$\left[\nabla\times\frac{1}{\sigma d}(\nabla\psi_1\times\mathbf{n} - \nabla\psi_2\times\mathbf{n})\right]\cdot\mathbf{n} = -(\mathbf{u}\cdot\nabla)(\mathbf{B}\cdot\mathbf{n}) \tag{8}$$

and T is no longer required. The magnetic scalar equations can be linked directly using $\mathbf{B}\cdot\mathbf{n}$. However care must be taken when solving such matrix systems which contain velocity diagonal entries only.

Verification

Results from the two new formulations are compared with those obtained from the more established moving $\mathbf{A}-\psi$ method, described and validated in [1]. The models are chosen such that the accuracy of the $\mathbf{A}-\psi$ method is not deteriorated by the aspect ratio of the elements. Two test problems involving DC currents have been found in the literature.

DC Current Moving Coil Experiment

The first experiment consists of a DC coil fixed over a spinning aluminium sheet which has been used for maglev research [4]. A linear model is illustrated in Fig. 2, the dimensions of which are listed in Table I.

The thin sheet is modelled using either $\mathbf{A}$, $T-\mathbf{B}\cdot\mathbf{n}$ or $\mathbf{B}\cdot\mathbf{n}$ formulations. A frequency of 0.1Hz was used for the $T-\mathbf{B}\cdot\mathbf{n}$ method, otherwise DC. The $\mathbf{A}$ method used contains an upwinding scheme [5]. The lift and drag force predictions are shown in Figs. 3 and 4, respectively.

In the sheet models, the sheet is located at the centre plane of the plate. All three computer model force results, all calculated using the method of Maxwell stress, agree with each other. The near constant discrepancy between the predicted and experimental forces, as can be

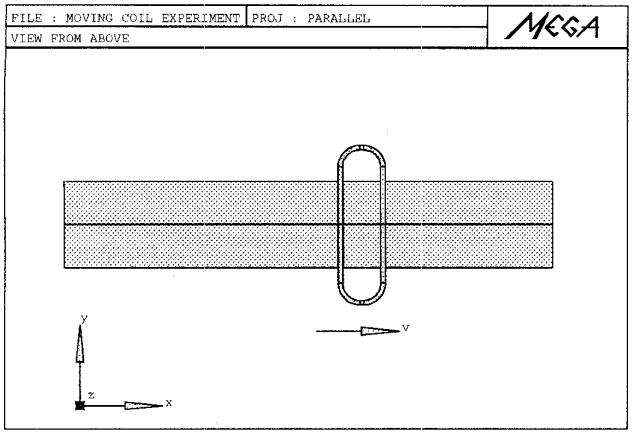

Fig. 2. Moving coil model

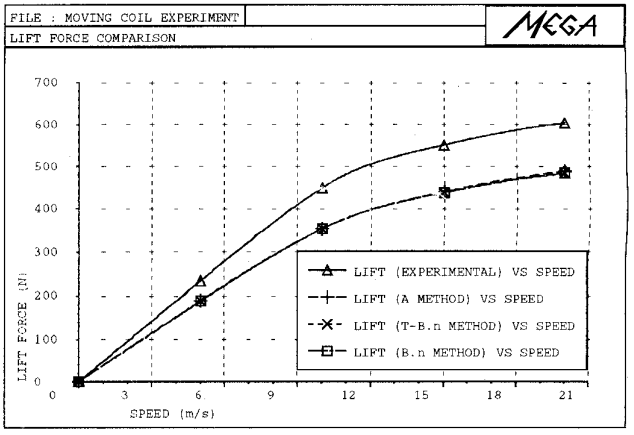

Fig. 3. Lift force results - moving coil experiment

TABLE I
Moving coil model parameters

sheet length	4.6m
sheet length for wake (from centre of coil)	2.8m
sheet width	0.8m
sheet thickness	10mm
conductivity of aluminium sheet	3.278E-7 S/m
coil length (outer dimensions)	0.441m
coil width (outer dimensions)	1.490m
height of coil windings	35mm
width of coil windings	41.5mm
internal radius of coil	0.169m
number of turns of coil	252
distance midsheet - midcoil	225mm
coil current	200A

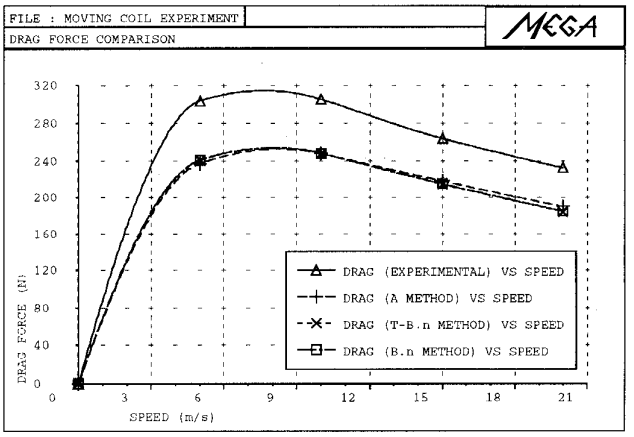

Fig. 4. Drag force results - moving coil experiment

seen in Tables II, III, and IV, cannot be clearly explained as yet. The thickness of the sheet was modelled by various discretisations of the **A** method and similar results were obtained, eliminating the possibility that the thin sheet approximation is invalid and causing the error. The drag force calculated from Joule heating is also shown on the tables and good agreement with Maxwell stress is obtained. However, a number of force comparisons for different separation distances between sheet and coil seem to indicate that the magnitude of forces is very sensitive to separation. For example, one particular change of 10mm in separation distance produced a variation of approximately 10% in forces. Therefore it is possible that the error is due to a misinterpretation of the model specification rather than a formulational difficulty. Graphs of $\mathbf{B}\cdot\mathbf{n}$ and current density vectors are shown in Figs. 5 and 6, respectively.

50 Hz Computer Model

Table V shows a comparison between the **A** and $T-\mathbf{B}\cdot\mathbf{n}$ methods for the model described in Table I at 50Hz. Good agreement is obtained for the AC moving case.

C-Core Magnet Experiment

This experiment, consisting of a C-core magnet moving over an aluminium sheet, is fully detailed in [1]. The frequency used for the $T-\mathbf{B}\cdot\mathbf{n}$ model is 1 Hz and the comparison between the the force predictions for the three formulations is shown in Fig. 7. The agreement between the three sets of computed forces is within 2%, while the maximum discrepancy with the experimental measurements is approximately 8%.

CONCLUSIONS

Two new formulations based on scalar variables are used to model thin moving sheets. Force and flux density predictions obtained using these schemes compare very favourably with the more usual moving $\mathbf{A}-\psi$ method. While a non negligible constant discrepancy with a specific set of experimental measurements is recognized, the error is most probably due to a misinterpretation in the model specifications rather than a formulational difficulty. The methods are further compared with a second test

TABLE II
Discrepancy between experiment and $\mathbf{A}$ method

Speed (m/s)	Lift force error (%) Maxwell stress	Drag force error (%) Maxwell stress	Drag force error (%) Joule heating
05	19.7	22.0	21.8
10	21.3	18.9	18.4
15	20.2	17.4	16.4
20	18.9	18.4	16.8

TABLE III
Discrepancy between experiment and $T - \mathbf{B} \cdot \mathbf{n}$ method

Speed (m/s)	Lift force error (%) Maxwell stress	Drag force error (%) Maxwell stress	Drag force error (%) Joule heating
05	20.4	20.8	21.4
10	21.2	18.8	18.3
15	20.6	18.7	18.8
20	19.9	20.8	20.4

problem and much closer agreement is obtained between computed and measured force results.

REFERENCES

[1] D.Rodger T.Karaguler and P.J.Leonard. "An optimal formulation for 3D moving eddy current problems with smooth rotors". *IEEE Trans. Mag.*, 26(5), Sept 1990.

[2] J.Simkin and C.W.Trowbridge. "On the use of the total scalar potential in the numerical solution of three dimensional magnetostatic problems". *IJNME*, 14:423–440, 1979.

[3] D.Rodger and N.Atkinson. "Finite element method for 3D eddy current flow in thin conducting sheets". *IEE Proceedings, Pt. A.*, 135(6):369–374, July 1988.

[4] B.T.Ooi D.L.Atherton, A.R.Eastham and O.P.Jain. "Forces and Moments for Electrodynamic Levitation Systems — Large-Scale Test Results and Theory". *IEEE Trans. on Magnetics*, 14(2):59–68, March 1978.

[5] T.J.R.Hughes. "A simple scheme for developing "upwind" finite elements". *IJNME*, 12:pp 1359–1365, 1978.

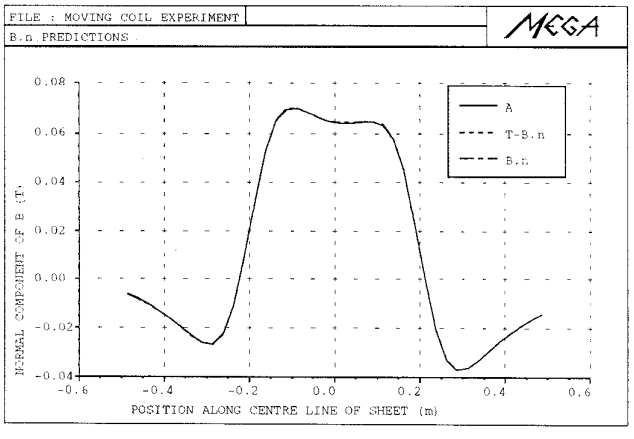

Fig. 5. Normal component of B along the middle of the sheet

TABLE IV
Discrepancy between experiment and $\mathbf{B} \cdot \mathbf{n}$ method

Speed (m/s)	Lift force error (%) Maxwell stress	Drag force error (%) Maxwell stress	Drag force error (%) Joule heating
05	20.1	20.8	21.7
10	21.3	18.8	19.3
15	20.6	18.5	19.4
20	19.9	20.6	21.4

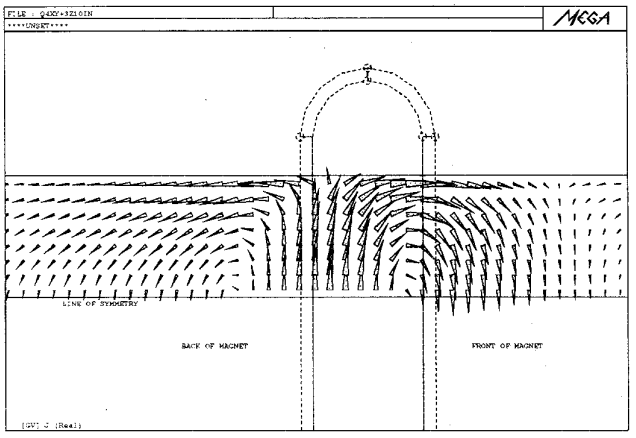

Fig. 6. Current density vectors on the sheet

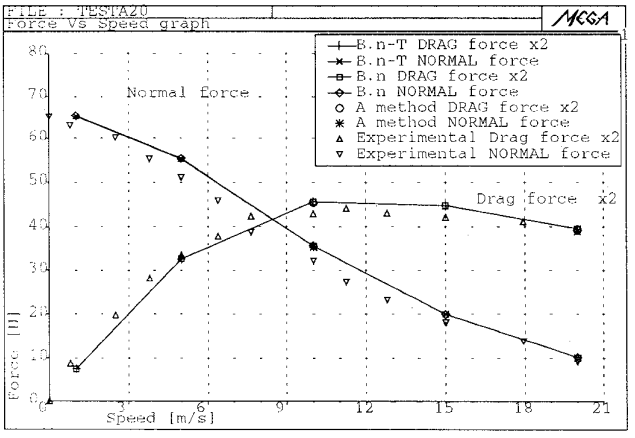

Fig. 7. Lift and drag forces

TABLE V
Discrepancy between $\mathbf{A} - \psi$ and $T - \mathbf{B} \cdot \mathbf{n}$ methods at 50Hz

Speed = 10m/s	Lift force (N)	Drag force (N)
$\mathbf{A} - \psi$	616.2	12.1
$T - \mathbf{B} \cdot \mathbf{n}$	588.8	11.5
Error (%)	4.4	5.0

Speed = 20m/s	Lift force (N)	Drag force (N)
$\mathbf{A} - \psi$	608.2	25.0
$T - \mathbf{B} \cdot \mathbf{n}$	582.8	25.4
Error (%)	4.2	1.6